# Experimental evidence of long-range magnetic order in the $c(2\times2)$ MnCu(100) surface alloy

Y. Huttel,[1] C. M. Teodorescu,[2] F. Bertran,[2] and G. Krill[2]
[1]*Instituto de Ciencia de Materiales, CSIC, 28049 Madrid, Spain*
[2]*LURE, Bâtiment 209D, Centre Universitaire Paris-Sud, 91 405 Orsay, France*
(Received 16 January 2001; published 2 August 2001)

The first experimental evidence of long-range magnetic order in the $c(2\times2)$MnCu(100) surface alloy formed by adsorption of 0.5 monolayer of Mn on Cu(100) at room temperature is reported. A carefully prepared $c(2\times2)$MnCu(100) surface alloy exhibits a clear x-ray magnetic circular dichroism (XMCD) signal at low temperatures. From the temperature behavior of the XMCD signal, we deduce a Curie temperature $T_c \approx 50$ K. As for other surfaces containing Mn, we demonstrate that the magnetic properties of the surface alloy are strongly affected by contamination.

DOI: 10.1103/PhysRevB.64.094405 PACS number(s): 75.70.Ak, 75.70.Rf

Surface magnetism may differ considerably from bulk magnetism. For instance, in the case of three-dimensional (3D) transition metals, the reduction of crystal field at surfaces, as well as the narrowing of *d* bands and the enhancement of the density of states at the Fermi level, can modify considerably the surface magnetic properties.[1–3] The understanding of surface magnetic properties is of fundamental importance but also mandatory for technological applications involving phenomena such as giant magnetoresistance, oscillatory interlayer coupling, spin injection, and high-density storage devices. Manganese and related compounds are of particular interest due to the high magnetic moment ($5\mu_B$) expected for Mn according to Hund's rules.

The $c(2\times2)$MnCu(100) ordered surface alloy is formed by room-temperature (RT) adsorption of 0.5 monolayer of Mn on Cu(100). The formation of this 50/50 ordered and truly 2D surface alloy is remarkable because no other CuMn intermetallic phase is known to exist (except for metastable and controversial $Cu_3Mn$, $Cu_5Mn$). The close relationship between the atomic structure and magnetism has converted the $c(2\times2)$MnCu reconstruction in one of the most investigated 2D magnetic compounds.[4–6] Its atomic structure has been investigated by different experimental techniques.[7–10] The Mn atoms occupy substitutional adsorption sites with a large outward corrugation [around 0.03 Å (Ref. 8)] that has been assigned to the high local magnetic moment of Mn atoms.[6,9,11] It is clear that the formation of a $c(2\times2)$Mn structure on Cu(100) attracted great interest, because of the larger interatomic distance between high-spin atoms, which generally leads to ferromagnetic (FM) ordering.[12]

The magnetism of the $c(2\times2)$MnCu surface alloy is still a challenge, since theoretical studies predict paramagnetism, antiferromagnetism (AFM), and ferromagnetism for the $c(2\times2)$MnCu surface alloy, and are in strong disagreement with experimental results.[2,4–6,9,11,13–15] The calculated magnetic moment in the $c(2\times2)$ ferromagnetic and face-centered-cubic configurations varies also from around 2.89 to 4.09 $\mu_B$,[2,4,5,13,15] which has to be compared with the experimental value for the atomic magnetic moment of a Mn impurity in Cu of 4.9 $\mu_B$.[16] Previous x-ray absorption experiments performed at Mn $L_{2,3}$ edges have reported a high-spin ground state for Mn.[6,14,17] However from x-ray magnetic circular dichroism (XMCD) experiments, performed at room temperature the absence of long-range magnetic order was concluded.[14] Further experiments performed between 70 and 300 K, yielded to the same conclusion.[5,6,9]

In this paper we report the first experimental observation of a long-range magnetic order of the $c(2\times2)$MnCu(100) surface alloy at low temperature. We clearly show that the $c(2\times2)$MnCu(100) reconstruction is magnetically long-range ordered below 50 K and that contamination of the surface has drastic consequences for the magnetic properties.

The experiments were performed on beamline SU23 at the storage ring superACO of LURE in Orsay. The samples were prepared in a molecular-beam-epitaxy installation that operates in the low $10^{-10}$ to $10^{-11}$ hPa range and is equipped with low-energy and reflectance high-energy electron diffraction (LEED and RHEED) and Auger spectroscopy (AES) facilities. Cu(100) single crystals were prepared by repeated cycles of sputtering and annealing. Manganese was evaporated from a well-outgassed Knudsen cell in a $10^{-10}$ hPa range at a rate of 1 Å/min, as measured by a water-cooled thickness monitor. As shown below, the contamination of the surface plays an important role in the magnetic properties. The present study has been performed on almost 30 carefully prepared surfaces. Repeated checking of the absence of contamination on the freshly prepared surface was performed by AES (mainly oxygen and carbon). Each sample was investigated by LEED prior to XMCD measurements and all measured surfaces presented well-defined $c(2\times2)$ reconstructions. Figure 1 presents a typical LEED pattern obtained for the clean Cu(100) substrate and after RT deposition of 0.5 monolayer of Mn.

After preparation, the samples were transferred under

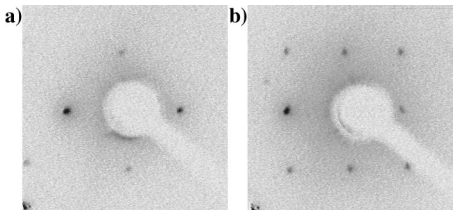


FIG. 1. (a) LEED pattern of the clean Cu(100) surface and (b) of the $c(2\times2)$Mn/Cu(100) surface alloy. The primary electron beam energy was 120 eV. The gray scale of the images was inverted: darkest-spots correspond to the most-intense diffraction spots.

 

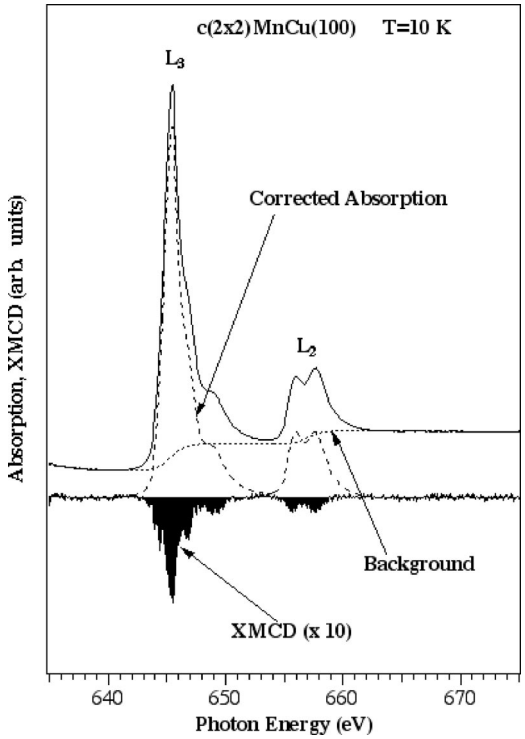


FIG. 2. Absorption spectra at the Mn $L_2$ and $L_3$ edges together with XMCD-spectra measured on the $c(2\times2)$MnCu(100) surface alloy at 10 K. Top spectra: absorption spectra with the step function used for the background subtraction and background spectrum. Bottom spectra: x-ray magnetic circular dichroism spectrum (see text for details).

vacuum into the analysis chamber connected to the SU23 beamline. The XMCD experiments were performed in the analysis chamber using a 60% circularly polarized light and in the $10^{-11}$ hPa pressure range. The data acquisition was performed using different geometries (changing the angle of photon incidence) and recording the total electronic yield (TEY) of the sample when excited with soft x rays. The direction of the applied magnetic field (1 T) was horizontal and parallel to the incident photon beam and the orientation of the magnetic field was reversed between two-successive absorption spectra. The sample was mounted vertically in such a way that the surface normal was included in the horizontal plane and the [11] direction of the sample surface oriented at 45° with respect to the horizontal plane.

Figure 2 represents the absorption spectra at the Mn $L_2$ and $L_3$ edges corresponding to the $c(2\times2)$MnCu(100) surface alloy together with the background curve (which takes into account the transitions from the core-level states to the continuum[18]), the background-corrected absorption spectrum and the corresponding XMCD spectrum.

The observation at $T=10$ K of an XMCD signature at the Mn edge in Fig. 2 is the experimental evidence that a long-range ordered ferromagnetic component is present in the $c(2\times2)$MnCu surface alloy. It is important to note that magnetic field effects on the TEY signal and possible saturation effects due to nonideal geometry have been carefully taken into account;[19] measurements in the remanent configuration and with different geometries on almost 30 samples

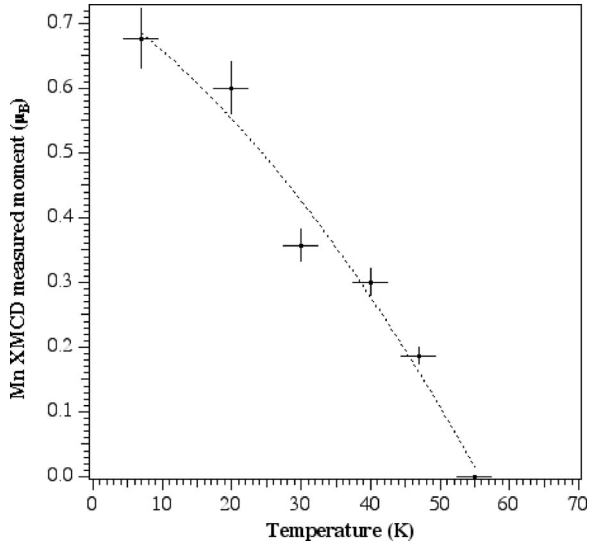


FIG. 3. Mn-magnetic-moment variation with temperature. The magnetic moment has been derived from the integrated $L_3$ XMCD signal as indicated in the text.

have given similar spectra. Even though we have achieved our main goal by demonstrating the existence of a long-range magnetic ordering of the $c(2\times2)$MnCu(100) surface alloy at low temperature, several questions must still be answered like those related to the shape of the XMCD signal or to the exact value of the magnetic moment itself; these points will be discussed in more detail below.

Furthermore the ferromagnetic origin of the XMCD signal on the 2D surface alloy is confirmed by the existence of a magnetic phase transition that is clearly observed in Fig. 3 where we display the temperature dependence of the Mn magnetic moment (the magnetic moment has been derived from the XMCD signal amplitude as explained below). The surface alloy presents a paramagnetic to ferromagnetic phase transition at a Curie temperature $T_c$ between 47 K (the highest temperature that provided an XMCD signal) and 55 K (where the XMCD signal was zero). As seen in Fig. 3, the temperature behavior of the magnetic moment in the low-temperature range ($T<20$ K) seems not to follow a $(T/T_c)^{\beta}$ with $\beta=3/2$ behavior, but rather the one often observed on ultrathin magnetic layers.[20] This is consistent with the two-dimensional nature of the $c(2\times2)$Mn/Cu(100) surface alloy. Near the Curie temperature, the present data do not allow a precise determination of the critical exponent $\beta$, but nevertheless, the behavior of the magnetic moment is still consistent with the values of $\beta$ obtained for ultrathin films.[21]

The shape of the XMCD signal of Mn, as reported in Fig. 2, is typical of the physical situations where the 3*d* electrons on the Mn atoms are rather localized. For instance, it compares very well with some of the XMCD spectra reported for Mn in the case of Mn/Fe(100).[22,23] As shown previously,[23,24] the presence of small amounts of oxygen on surfaces can strongly modify the magnetic properties. Since the contamination of the surface (mainly due to oxygen) is an important issue for the present study, we discuss in the last section of our paper the effect of contamination on the XMCD signal.

However we present now an estimation of the magnetic

TABLE I. Magnetic moments for the Mn atoms in the $c(2\times2)$MnCu surface alloy for the present work and calculated assuming a ferromagnetic configuration.

| $\mu$ ($\mu_B$) | 3.5 | 3.75 | 4.09 | 3.85 | $0.67\pm0.08$ |
|---|---|---|---|---|---|
| References | 13 Theory | 5 Theory | 4 Theory | 15 Theory | This work Experiment |

moment. Taking into account the well-known fact that the sum rules (especially the second one used to derive the value of $\langle Sz\rangle$), cannot be applied to the Mn $L_{2,3}$ edges, we prefer to estimate the magnetic moments by comparing the present XMCD amplitude with those available in the literature. The $L_3$ XMCD signal amplitude in our case (uncorrected by the circular polarization factor of 0.6) represents 3.2% of the absorption signal. In the case of fcc Mn/Co(001) system, 36% of XMCD (corrected) signal was assigned to 4.5 $\mu_B$, which gives a value of 8% XMCD for 1 $\mu_B$.[25] For the bcc Mn/Fe(001) systems, the following percentages of XMCD per $\mu_B$ have been reported: 8.8% XMCD/$\mu_B$ (Ref. 22), 9.2%/$\mu_B$ (Ref. 23), and 7.4% XMCD/$\mu_B$.[26] Assuming that an average value of $8\pm1\%$ $L_3$ XMCD signal corresponds to 1 $\mu_B$, and taking into account the polarization of the beamline, we obtain from our spectra a magnetic moment for Mn atoms of $0.67\pm0.08$ $\mu_B$. The resulting Mn moment is still small when compared with that calculated (see Table I) and to its high-spin value derived from x-ray absorption spectra that is around $4.5\mu_B$.[6,14,17,26] The experiments presented in Fig. 2 were performed at 10 K, i.e., well below the Curie temperature (see Fig. 3). Therefore the small value of the magnetic moment is not due to the temperature effect.

In the following possible origins of the small value of the measured moment will be discussed: (i) traces of contamination that reduce the magnetism of the surface (mainly oxygen);[23,27] (ii) the Mn atoms are not ferromagnetically but ferrimagnetically ordered, owing to a competition between FM and AFM ground states.[4,28]

The influence of contamination on the magnetism of the $c(2\times2)$MnCu(100) alloy is clearly observable in Figs. 4 and 5. Figure 4 displays the evolution of the absorption spectra at the Mn $L_{2,3}$ edges and corresponding XMCD signals vs time (i.e., contamination). It can be clearly observed that the change in the shape of the absorption spectra is followed by a reduction of the intensity of the $L_3$ XMCD amplitude as a function of time. Upon time the shape of the absorption spectra becomes more structured, which is an indication of surface contamination as already reported.[23] The surface contamination induces a drastic reduction of the $L_3$ integrated XMCD amplitude as can be observed in Fig. 5.

The very fast decay of the $L_3$ integrated XMCD amplitude with time gives an indication of the difficulty of the present measurements. Even in the $10^{-11}$ hPa pressure range, the surface is rapidly contaminated mainly due to the high sticking coefficient of residual-gas molecules on the cold surface. Freshly-prepared samples did not show any oxygen peak in AES, but showed well-defined $c(2\times2)$ reconstructions and unstructured absorption spectra, characteristic for a metallic state (see left upper inset of Fig. 5). On the other hand, after few hours of measurements, the XMCD signal disappeared and the spectra became peaked, characteristic for multiplet spectra of manganese oxides (see right upper inset of Fig. 5). Furthermore the contaminated surfaces showed traces of oxygen in AES spectra and no $c(2\times2)$ LEED diagram. The magnetic moment of $0.67\pm0.08$ $\mu_B$

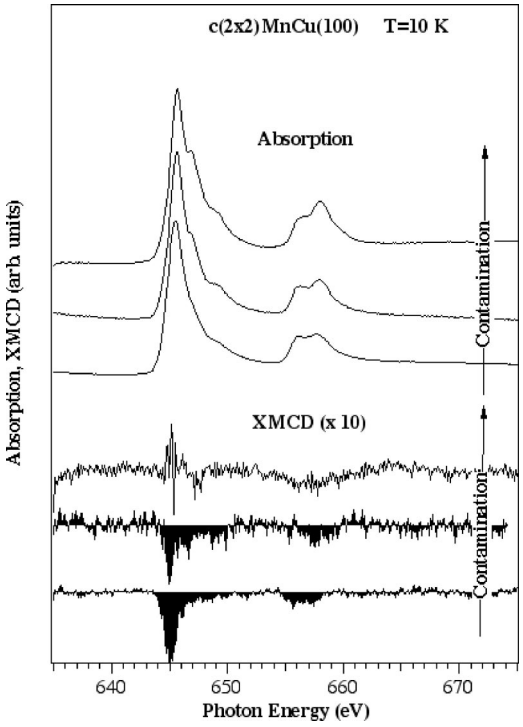


FIG. 4. Absorption spectra at the Mn $L_{2,3}$ edges and the corresponding XMCD signal as a function of time, i.e., contamination of the surface.

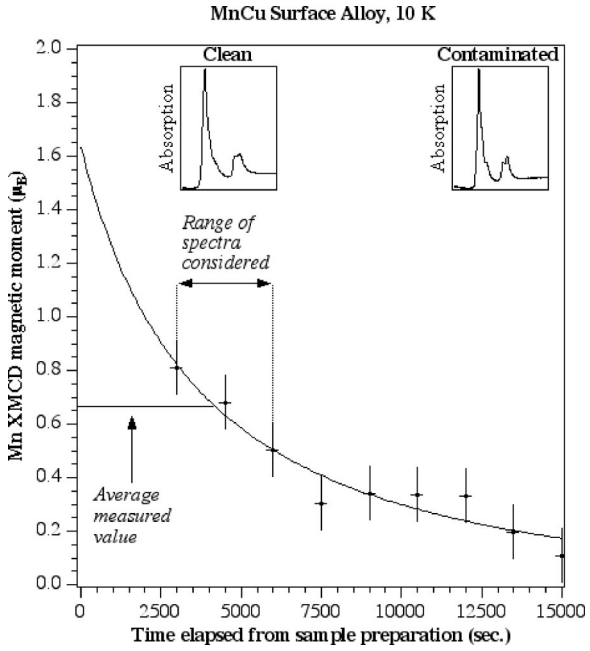


FIG. 5. Magnetic moment as a function of time, i.e., contamination of the surface.

has been extracted from spectra mesured in the time range from $t=2600$ s to $t=5200$ s as indicated in Fig. 5. The time range from $t=0$ s to $t=2600$ s corresponds to the time needed to transfer the sample from the preparation chamber to the analysis chamber and to cool down the sample. We have estimated the expected Mn magnetic moment for an ideally clean surface (i.e., at t=0 s) by assuming that the contamination process is exponential with time.[29] The experimental data points have been fitted with the following formula $f(t)=A/[1+b(e^{t/\tau}-1)]$, where $A$ represents the XMCD normalized signal in absence of contamination, $b$ the ratio between the oxide and the metallic-Mn cross sections (the absorption cross section of oxides is larger than that of metals), and $\tau$ the lifetime of the surface. The parameters obtained for the curve-fit displayed in Fig. 5 are $A=1.63\pm0.25\mu_B$ (to be compared with the average value of 0.67 $\mu_B$ over the time range of measurement), $b=3.68$, and $\tau=16\,300$ s (very close to what one expects to be the contamination lifetime of half a monolayer in the $10^{-11}$ hPa pressure range). Consequently it is reasonable to expect a factor of 2.6 between the measured XMCD signal and the signal expected from an ideally uncontaminated surface. The expected magnetic moment would be therefore close to 1.7 $\mu_B$. Since the experimental magnetic moment is still well below the theoretical values (see Table I) and measured local magnetic-moment values[25] (on the order of 4.5 $\mu_B$), one can reasonably question whether or not the present theoretical models give an accurate description of the $c(2\times2)$MnCu surface alloy and if the long-range magnetic order is not ferromagnetic but ferrimagnetic.

In conclusion, we have observed for the first time the long-range magnetic ordering of the $c(2\times2)$MnCu(100) surface alloy. The experimental data have given clear evidence of the magnetic-phase transition from paramagnetic to ferromagnetic (ferrimagnetic) configurations with a Curie temperature $T_c=50\pm5$ K and a temperature behavior that is typical of that observed in ultrathin films. We have also shown that contamination modifies the magnetic properties of the surface reconstruction reducing drastically the magnetic moment. Taking into account such effect we have derived an experimental magnetic moment that does not exceed 1.7 $\mu_B$. This magnetic moment is much lower (about one-third) than the moments predicted by calculations and expected from the local high-spin magnetic moment of manganese derived from $L_{2,3}$ absorption branching ratio suggesting that the $c(2\times2)$MnCu(100) surface alloy could also be ferrimagnetic.

This work has been partially financed by Ministerio de Educación y Cultura, España, and by University of York, United Kingdom.

[1] H. Krakauer, A.J. Freeman, and E. Wimmer, Phys. Rev. B **28**, 610 (1983); C.L. Fu, A.J. Freeman, and T. Oguchi, Phys. Rev. Lett. **54**, 2700 (1985); C.M. Schneider, P. Bressler, J. Kirschner, J.J. de Miguel, and R. Miranda, *ibid.* **64**, 1059 (1990); G. van der Laan, M.A. Hoyland, M. Surman, C.F.J. Flipe, and B.T. Thole, *ibid.* **69**, 3827 (1992).

[2] O. Ericksson, A.M. Boring, R.C. Albers, G.W. Fernando, and B.R. Cooper, Phys. Rev. B **45**, 2868 (1992).

[3] M. Tischer, O. Hjortstam, D. Arvantis, J. Hunter Dunn, F. May, K. Baberschke, J. Trygg, J.M. Wills, B. Johansson, and O. Eriksson, Phys. Rev. Lett. **75**, 1602 (1995).

[4] M. Eder, J. Hafner, E.G. Moroni, Phys. Rev. B **61**, 11 492 (2000).

[5] O. Rader, W. Gudat, C. Carbone, E. Vescovo, S. Blgel, R. Klsges, W. Eberhardt, M. Wuttig, J. Redinger, and F.J. Himpsel, Phys. Rev. B **55**, 5404 (1997).

[6] W.L. O'Brien and B.P. Tonner, Phys. Rev. B **51**, 617 (1995).

[7] T. Flores, M. Hansen, and M. Wuttig, Surf. Sci. **279**, 251 (1992).

[8] M. Wuttig, C.C. Knight, T. Flores, and Y. Gauthier, Surf. Sci. **292**, 189 (1993).

[9] M. Wuttig, Y. Gauthier, and S. Blügel, Phys. Rev. Lett. **70**, 3619 (1993).

[10] C. Binns and C. Norris, Surf. Sci. **116**, 338 (1982); R.G.P. van der Kraan and H. van Kempen, *ibid.* **338**, 19 (1995); W.F. Egelhoff, Jr., I. Jacob, J.M. Rudd, J.F. Cochran, and B. Heinrich, J. Vac. Sci. Technol. A **8**, 1582 (1990).

[11] M. Wuttig, B. Feldmann, and T. Flores, Surf. Sci. **331-333**, 659 (1995).

[12] M. Albrecht *et al.*, Phys. Rev. Lett. (to be published).

[13] S. Blügel, Appl. Phys. A: Mater. Sci. Process. **63**, 595 (1996).

[14] W.L. O'Brien, J. Zhang, and B.P. Tonner, J. Phys.: Condens. Matter **5**, L515 (1993).

[15] D. Wortmann, S. Heinze, G. Bihlmayer, and S. Blügel, Phys. Rev. B **62**, 2862 (2000).

[16] J.D. Cohen and C.P. Slichter, Phys. Rev. B **22**, 45 (1980).

[17] Y. Huttel, F. Schiller, J. Avila, and M.C. Asensio, Phys. Rev. B **61**, 4948 (2000).

[18] Joachim Stöhr, *NEXAFS Spectroscopy*, Spinger Series in Surface Sciences Vol. 25 (Springer-Verlag, Berlin, 1992).

[19] W.L. O'Brien and B.P. Tonner, Phys. Rev. B **50**, 12 672 (1994).

[20] See, for example, D. Pescia, M. Stampanoni, G.L. Bona, A. Vaterlaus, R.F. Willis, and F. Meier, Phys. Rev. Lett. **58**, 2126 (1987).

[21] H.C. Siegmann, J. Phys.: Condens. Matter **4**, 8395 (1992).

[22] S. Andrieu, M. Finazzi, Ph. Bauer, H. Fischer, P. Lefevre, A. Traverse, K. Hricovini, G. Krill, and M. Piecuch, Phys. Rev. B **57**, 1985 (1998).

[23] S. Andrieu, E. Foy, H. Fischer, M. Alnot, F. Chevrier, G. Krill, and M. Piecuch, Phys. Rev. B **58**, 8210 (1998).

[24] W.L. O'Brien and B.P. Tonner, Phys. Rev. B **58**, 3191 (1998).

[25] W.L. O'Brien and B.P. Tonner, Phys. Rev. B **50**, 2963 (1994).

[26] J. Dresselhaus, D. Spanke, F.U. Hillebrecht, E. Kisker, G. van der Laan, J.B. Goedkoop, and N.B. Brookes, Phys. Rev. B **56**, 5461 (1997).

[27] F. Passek and M. Donath, Phys. Rev. Lett. **71**, 2122 (1993).

[28] R. Wu and A.J. Freeman, Phys. Rev. B **51**, 17 131 (1995).

[29] C. M. Teodorescu, Ph.D. thesis, *Photoabsorption X*, Université Paris Sud, 1995.